COHERENT EFFECTS IN THE MULTIPLE SCATTERING OF LIGHT IN RANDOM MEDIA

E. AKKERMANS
Department of Physics, Technion, 32000 Haifa, Israel

AND

G. MONTAMBAUX
Laboratoire de physique des solides, Université Paris-Sud F-91405 Orsay Cedex, France

Abstract. We review some of the characteristic features of the coherent multiple scattering of scalar electromagnetic waves in random media. The probability of quantum diffusion is defined and calculated up to the contribution of the cooperon. We show that there are additional corrections at the order of the cooperon which restore the normalization of the probability. We study also the angular and temporal (diffusive wave spectroscopy) correlation functions of speckle patterns. More particularly, we obtain a closed expression of the contribution to the time correlation function which is equivalent to the universal conductance fluctuations. Finally, the notion of dephasing is discussed and implemented for the case of the dephasing induced by the internal Zeeman degrees of freedom of cold atomic gases.

1. Introduction

This contribution aims to give a general survey of the field of coherent multiple scattering of light by random media. This field crosses through many topics in physics. Nevertheless, apart from details which are specific to each particular physical problem, there is a large amount of common features which characterize coherent multiple scattering of waves ranging from mesoscopic metals to astrophysics. A unified description of the basic features of coherent multiple scattering have been presented elsewhere [1, 2]. In this short review, we shall mostly focus on the behavior of elec-

B.A. van Tiggelen and S.E. Skipetrov (eds.),
Wave Scattering in Complex Media: From Theory to Applications, 101–124.

tromagnetic waves scattering either in suspensions of classical scatterers or in quantum systems such as cold atomic gases.

In the next section we shall describe two models for randomness which are most frequently used and discuss their relation with the cross section of an individual scatterer. Then, we shall review the main results about the disorder average amplitude in multiple scattering in the weak scattering limit. A central quantity which is ubiquitous in all the physical results is *the probability of quantum diffusion*. We shall discuss it quite in details and subsequently apply it to the study of correlation functions in speckle patterns, the time correlation function in the multiple scattering limit (diffusive wave spectroscopy) and to a discussion of some processes leading to dephasing *i.e.* to the existence of a finite phase coherence time in the multiple scattering of photons by cold atomic gases. We shall then discuss this kind of dephasing and compare it to other mechanisms in mesoscopic metallic systems.

2. Scalar Waves in Random Media

We consider an electromagnetic wave which propagates in a non dissipative and non magnetic heterogeneous dielectric medium characterized by the real and positive dielectric constant $\epsilon(\mathbf{r}) = \bar{\epsilon} + \delta\epsilon(\mathbf{r})$. It fluctuates around the average value $\bar{\epsilon}$. By writing the corresponding Maxwell equations, we obtain a wave equation for the electric field. In a first step, we shall disregard the polarization of the field and consider the case of a scalar electric field described by the complex function $\psi(\mathbf{r})$ and solution of the Helmholtz equation

$$-\Delta\psi(\mathbf{r}) - k_0^2\mu(\mathbf{r})\psi(\mathbf{r}) = k_0^2\psi(\mathbf{r}) \tag{1}$$

The quantity $\mu(\mathbf{r}) = \delta\epsilon/\bar{\epsilon}$ is the relative fluctuation of the dielectric constant and $k_0 = \bar{n}\omega/c$ where $\bar{n} = \sqrt{\frac{\bar{\epsilon}}{\epsilon_0}}$ is the average refraction index. This equation is similar to the Schrödinger equation for a free particle in a potential $V(\mathbf{r})$. Here, the disorder potential is $V(\mathbf{r}) = -k_0^2\mu(\mathbf{r})$. It is proportional to the square of the frequency so that, unlike electronic systems, a lowering of the frequency leads to a weaker effect of the disorder. The disorder potential is a random and continuous function of the position. We can choose the origin of the energies so that $\langle V(\mathbf{r})\rangle = 0$ where $\langle\cdots\rangle$ accounts for the average over the configurations of the disorder. A simple approximation consists in assuming that $V(\mathbf{r})$ is a Gaussian random variable. Therefore, only the second cumulant does not vanish. Moreover, we shall assume that the wavelength is much larger than the correlation length of the potential so that the two-point correlation function may be written as

$$\langle V(\mathbf{r})V(\mathbf{r}')\rangle = B\delta(\mathbf{r} - \mathbf{r}') \tag{2}$$

where B is a constant. This model corresponds to the so-called white noise limit.

The white noise model does not contain information about the microscopic nature of the disorder. Another model first introduced by Edwards [3] describes the disorder potential as a collection of N_i identical localized scatterers each of them characterized by the scattering potential $v(\mathbf{r})$, namely

$$V(\mathbf{r}) = \sum_{j=1}^{N_i} v(\mathbf{r} - \mathbf{r}_j) \quad . \tag{3}$$

The density $n_i = \frac{N_i}{\Omega}$ is taken to be constant in the limit $\Omega \to \infty$. We shall moreover consider the scattering potential $v(\mathbf{r})$ to be central and short range, *i.e.*, $v(\mathbf{r} - \mathbf{r}_j) = v_0 \delta(\mathbf{r} - \mathbf{r}_j)$. In the limit of large densities $n_i \to \infty$ of weak scatterers $v_0 \to 0$ but with a constant value for $n_i v_0^2$, the Edwards model is equivalent to the white noise model provided we have the equality $B = n_i v_0^2$.

The total cross section is given, in the Born approximation, by $\sigma = v_0^2/4\pi$, so that the parameter B of the white noise model is simply related to the cross section of an individual scatterer:

$$B = 4\pi n_i \sigma \tag{4}$$

However, it is important to keep in mind the following point. In order to obtain the Edwards limit of a δ potential, we must consider the limits of both an infinite strength U_0 and a vanishing range b so that the combination $v_0 = 4\pi b^3 U_0/3$ is constant. Strictly speaking, the Born approximation breaks down in this limit. However, in the limit of a white noise model where $v_0 \to 0$, the Born approximation remains valid.

3. The Average Amplitude of a Multiply Scattered Wave

In the presence of sources $j(\mathbf{r})$ of the electric field, the solutions of the Helmholtz equation (1) may be written,

$$\psi(\mathbf{r}) = \int d\mathbf{r}_i j(\mathbf{r}_i) G(\mathbf{r}_i, \mathbf{r}, k_0) \tag{5}$$

where the Green function $G(\mathbf{r}_i, \mathbf{r}, k_0)$ is solution of [4]

$$\left(\Delta_{\mathbf{r}} + k_0^2(1 + \mu(\mathbf{r}))\right) G(\mathbf{r}_i, \mathbf{r}, k_0) = \delta(\mathbf{r} - \mathbf{r}_i) \tag{6}$$

This Green function can be expressed in terms of the free Green function G_0 solution of the previous equation but in the absence of the scattering

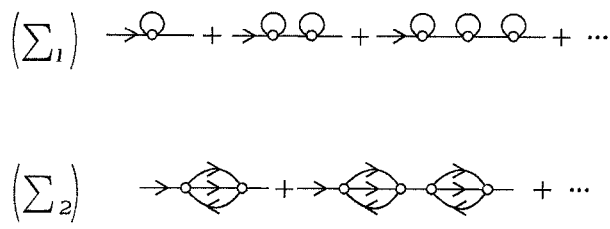

Figure 1. Series of terms respectively generated by Σ_1 and Σ_2 in the self-energy.

potential, *i.e.*, for $\mu(\mathbf{r}) = 0$,

$$G(\mathbf{r}_i, \mathbf{r}, k_0) = G_0(\mathbf{r}_i, \mathbf{r}, k_0) - k_0^2 \int d\mathbf{r}' G(\mathbf{r}_i, \mathbf{r}', k_0)\mu(\mathbf{r}')G_0(\mathbf{r}', \mathbf{r}, k_0) \qquad (7)$$

It is possible to write a formal multiple scattering expansion by iterating the previous relation. By taking the average over a white noise potential, we restore the translational invariance, so that the Fourier transform of the average Green function can be written

$$\overline{G}(\mathbf{k}) = G_0(\mathbf{k}) + \overline{G}(\mathbf{k})\Sigma(\mathbf{k}, \epsilon)G_0(\mathbf{k}) \qquad (8)$$

The function $\Sigma(\mathbf{k}, \epsilon)$ is called the self-energy and it represents the sum of all the irreducible scattering events.

The perturbative expansion of the self-energy is in terms of the parameter $n_i v_0^2$. For weak scattering the main contribution is obtained by keeping only the first contribution Σ_1 in Fig. 1. The imaginary part of the corresponding expression of the self-energy defines the elastic mean free path l_e, namely

$$\frac{1}{l_e} = -\frac{1}{k_0}\mathrm{Im}\Sigma_1(\mathbf{k}, k_0) = n_i\sigma \qquad (9)$$

where σ is the cross section defined in (4). The first neglected term Σ_2 in Fig. 1 gives a correction

$$\mathrm{Im}\Sigma_2(k) = \frac{\pi}{2kl_e}\mathrm{Im}\Sigma_1(k) \qquad (10)$$

Hence, it allows to identify the small dimensionless parameter $1/k_0 l_e$ which characterizes the weak scattering limit that we shall consider all along this

paper. By keeping only the contribution of Σ_1, we neglect all the interference effects between scatterers (see Fig. 1).

Inserting (9) into (8) and performing a Fourier transform, one finds that the average Green function is given by

$$\overline{G}(\mathbf{r}_i, \mathbf{r}, \epsilon) = G_0(\mathbf{r}_i, \mathbf{r}, \epsilon) \; e^{-|\mathbf{r}-\mathbf{r}_i|/2l_e} = -\frac{e^{ik_0 R}}{4\pi R} \; e^{-R/2l_e} \tag{11}$$

where $R = |\mathbf{r} - \mathbf{r}_i|$. This expression corresponds to the retarded average Green function. The advanced one is obtained by changing the sign of k_0 in the previous expression.

4. The Probability of Quantum Diffusion

The quantities of physical interest are usually related not to the average Green function but instead to the so-called *probability of quantum diffusion* $P(\mathbf{r}, \mathbf{r}', t)$ for a wave packet to propagate between the points $\mathbf{r}$ and $\mathbf{r}'$ in a time t. The average over the disorder of the Fourier transform of this probability is given by [1, 2]

$$P(\mathbf{r}, \mathbf{r}', \omega) = \frac{4\pi}{c} \overline{G^R(\mathbf{r}, \mathbf{r}', \omega_0) G^A(\mathbf{r}', \mathbf{r}, \omega_0 - \omega)} \tag{12}$$

This probability is normalized to unity, namely

$$\int P(\mathbf{r}, \mathbf{r}', t) d\mathbf{r}' = 1 \tag{13}$$

or equivalently

$$\int P(\mathbf{r}, \mathbf{r}', \omega) d\mathbf{r}' = \frac{i}{\omega} \tag{14}$$

Three main contributions do appear in the probability $P(\mathbf{r}, \mathbf{r}', t)$:

- the probability to propagate between $\mathbf{r}$ and $\mathbf{r}'$ without scattering.
- the probability to propagate between $\mathbf{r}$ and $\mathbf{r}'$ by an incoherent sequence of multiple scattering. We shall call *diffuson* this contribution.
- the probability to go from $\mathbf{r}$ to $\mathbf{r}'$ by a coherent multiple scattering sequence. We shall call *cooperon* this coherent contribution to the probability.

The first contribution is obtained by replacing in (12) the average over the product of the two Green functions by the product of the averaged Green functions. This contribution known as the Drude-Boltzmann term rewrites as

$$P_0(\mathbf{r}, \mathbf{r}', \omega) = \frac{e^{i\omega R/c - R/l_e}}{4\pi R^2 c} \tag{15}$$

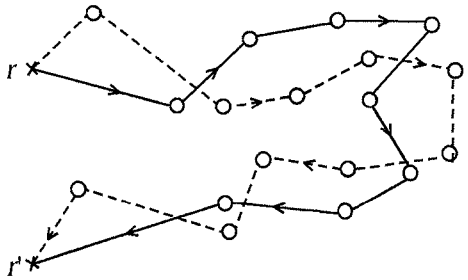

Figure 2. Typical trajectories associated respectively to the retarded (G^R) (solid line) and advanced (G^A) (dashed line) Green functions.

where c is the group velocity of the wave. It appears clearly that, at this approximation, the average probability is not normalized.

4.1. THE DIFFUSON

The second contribution to the probability accounts for multiple scattering in the weak disorder limit $kl_e \gg 1$. Following the previous description of the average Green function, we associate to each possible sequence $\mathcal{C}$ of independent effective collisions (Fig. 2) a complex amplitude $A(\mathbf{r}, \mathbf{r}', \mathcal{C})$. Hence, the Green function is given by the sum of such complex amplitudes [5].

In order to evaluate the probability which appears as a product of two Green functions, we notice first the following two points:

- due to the short range of the scattering potential, the set of scatterers entering in the multiple scattering sequences for both G^R and G^A must be identical.
- the average distance between two elastic collisions is set by the elastic mean free path $l_e \gg \lambda$. Therefore, if any two scattering sequences differ by even one collision event, the phase difference between the two complex amplitudes, which measures the difference of path lengths in units of λ will be very large and then the corresponding probability will vanish on average.

Therefore, we shall retain only the contributions of the type represented in

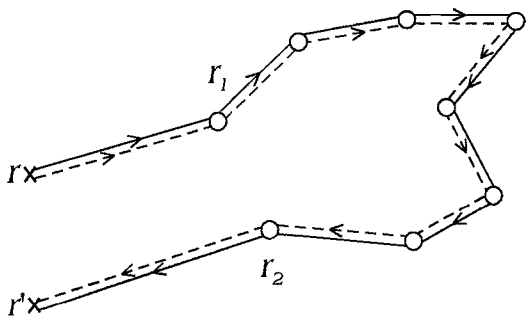

Figure 3. Multiple scattering trajectories which contribute to the average $\overline{G^R G^A}$.

Fig. 3 for which the corresponding probability $P_d(\mathbf{r}, \mathbf{r}', \omega)$ is

$$P_d(\mathbf{r}, \mathbf{r}', \omega) = \frac{4\pi}{c} \int \overline{G}^R_\epsilon(\mathbf{r}, \mathbf{r}_1) \overline{G}^A_{\epsilon-\omega}(\mathbf{r}_1, \mathbf{r}) \overline{G}^R_\epsilon(\mathbf{r}_2, \mathbf{r}') \overline{G}^A_{\epsilon-\omega}(\mathbf{r}', \mathbf{r}_2) \times \Gamma_\omega(\mathbf{r}_1, \mathbf{r}_2) d\mathbf{r}_1 d\mathbf{r}_2 \quad (16)$$

This expression involves two contributions. The first one

$$\overline{G}^R_\epsilon(\mathbf{r}, \mathbf{r}_1) \overline{G}^R_\epsilon(\mathbf{r}_2, \mathbf{r}') \overline{G}^A_{\epsilon-\omega}(\mathbf{r}_1, \mathbf{r}) \overline{G}^A_{\epsilon-\omega}(\mathbf{r}', \mathbf{r}_2)$$

describes the average propagation between any two points $\mathbf{r}$ and $\mathbf{r}'$ of the medium and the first ($\mathbf{r}_1$) (respectively the last ($\mathbf{r}_2$)) collision event of the multiple scattering sequence. The second contribution defines $\Gamma_\omega(\mathbf{r}_1, \mathbf{r}_2)$ which we shall call the average *structure factor* of the scattering medium. In a sense, it generalizes to the multiple scattering situation the usual two-point correlation function in the single scattering case. Relying again on the assumption of independent collisions allows to write for $\Gamma_\omega(\mathbf{r}_1, \mathbf{r}_2)$ the integral equation

$$\Gamma_\omega(\mathbf{r}_1, \mathbf{r}_2) = \frac{4\pi}{l_e} \delta(\mathbf{r}_1 - \mathbf{r}_2) + \frac{4\pi}{l_e} \int \overline{G}^R_\epsilon(\mathbf{r}_1, \mathbf{r}) \overline{G}^A_{\epsilon-\omega}(\mathbf{r}, \mathbf{r}_1) \Gamma_\omega(\mathbf{r}, \mathbf{r}_2) d\mathbf{r} \quad (17)$$

This equation can be solved exactly for some geometries. For the infinite three dimensional space, we obtain for the structure factor the expression

$$\Gamma_\omega(\mathbf{q}) = \frac{4\pi}{l_e} \frac{1}{1 - P_0(\mathbf{q}, \omega)/\tau_e} \quad (18)$$

where $P_0(\mathbf{q},\omega)$ is the Fourier transform of (15) and it is given by $\frac{1}{qv}$ arctan $\frac{ql_e}{1-i\omega\tau_e}$ with $q=|\mathbf{q}|$. The resulting probability thus rewrites

$$P_d(\mathbf{q},\omega)=P_0(\mathbf{q},\omega)\frac{P_0(\mathbf{q},\omega)/\tau_e}{1-P_0(\mathbf{q},\omega)/\tau_e} \tag{19}$$

We shall call *diffuson* this expression of the probability. The normalization of the total probability $P=P_0+P_d$ can be readily checked namely $P(\mathbf{q}=0,\omega)=\frac{i}{\omega}$.

In the hydrodynamic limit of slow spatial and temporal variations, *i.e.*, for $|\mathbf{r}-\mathbf{r}_2|\gg l_e$ and $\omega\tau_e\ll 1$, the integral equation (17) for Γ_ω simplifies and is solution of the diffusion equation

$$[-i\omega-D\Delta_{\mathbf{r}_1}]\,\Gamma_\omega(\mathbf{r}_1,\mathbf{r}_2)=\frac{4\pi c}{l_e^2}\delta(\mathbf{r}_1-\mathbf{r}_2) \tag{20}$$

where $D=\frac{1}{d}\frac{l_e^2}{\tau_e}=\frac{1}{d}v^2\tau_e$ is the diffusion coefficient. At this approximation, P_d and Γ_ω are related by

$$P_d(\mathbf{r},\mathbf{r}',\omega)\simeq\frac{l_e^2}{4\pi c}\Gamma_\omega(\mathbf{r},\mathbf{r}') \tag{21}$$

so that P_d, as well, obeys a diffusion equation.

4.2. THE COOPERON

The two previous contributions, namely the Drude-Boltzmann term and the diffuson which takes into account multiple scattering, provide a normalized expression of the probability. Therefore, we may think having exhausted all the contributions. But, consider now the multiple scattering sequences like those represented in Fig. 4. It corresponds to the product of Green functions of the kind we have considered before. But now the two identical trajectories are time reversed. It is clear that if these trajectories are closed on themselves, there is no phase difference left between them. This requires time-reversal invariance namely $G^{R,A}(\mathbf{r},\mathbf{r}',t)=G^{R,A}(\mathbf{r}',\mathbf{r},t)$. We shall call X_c the contribution of this process to the total probability. It can be evaluated as before and is given by

$$\begin{aligned}X_c(\mathbf{r},\mathbf{r}',\omega) &= \frac{4\pi}{c}\int\overline{G}^R_\epsilon(\mathbf{r},\mathbf{r}_1)\overline{G}^R_\epsilon(\mathbf{r}_2,\mathbf{r}')\overline{G}^A_{\epsilon-\omega}(\mathbf{r}',\mathbf{r}_1)\overline{G}^A_{\epsilon-\omega}(\mathbf{r}_2,\mathbf{r})\\ &\quad\times\Gamma'_\omega(\mathbf{r}_1,\mathbf{r}_2)d\mathbf{r}_1d\mathbf{r}_2\end{aligned} \tag{22}$$

In the case of time reversal invariance we have,

$$\overline{G}^R_\epsilon(\mathbf{r}_1,\mathbf{r})\overline{G}^A_\epsilon(\mathbf{r}_1,\mathbf{r})=\overline{G}^R_\epsilon(\mathbf{r}_1,\mathbf{r})\overline{G}^A_\epsilon(\mathbf{r},\mathbf{r}_1) \tag{23}$$

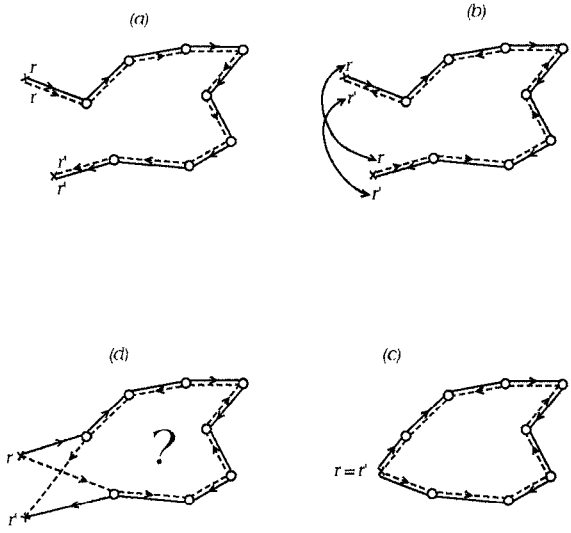

Figure 4. a) Classical contribution to the probability. b) By changing the direction of propagation of one of the trajectories there is still no overall dephasing provided that the two points $\mathbf{r}$ and $\mathbf{r}'$ coincide (c). d) If $\mathbf{r} \neq \mathbf{r}'$, there is a finite dephasing between the two trajectories.

so that the new structure factor $\Gamma'_\omega(\mathbf{r}_1, \mathbf{r}_2) = \Gamma_\omega(\mathbf{r}_1, \mathbf{r}_2)$. In the diffusion approximation, by calculating the integrals (16) and (22), we obtain

$$X_c(\mathbf{r}, \mathbf{r}', \omega) = P_d(\mathbf{r}, \mathbf{r}, \omega) \left(\frac{\sin kR}{kR} \right)^2 e^{-R/l_e} \tag{24}$$

with $R = |\mathbf{r} - \mathbf{r}'|$. For $R = 0$, *i.e.*, for $\mathbf{r} = \mathbf{r}'$, we have

$$X_c(\mathbf{r}, \mathbf{r}, \omega) = P_d(\mathbf{r}, \mathbf{r}, \omega) \tag{25}$$

namely, the probability to come back to the initial point is *twice* the value given by the diffuson. Nevertheless, it should be noticed that unlike the diffuson P_d and the structure factor Γ_ω, the cooperon X_c does not obey a diffusion equation.

4.3. NORMALIZATION OF THE QUANTUM PROBABILITY

We have seen that the contributions of both the Drude-Boltzmann term and the diffuson end up with a normalized probability of quantum diffusion. Therefore, it is expected that the additional contribution of the

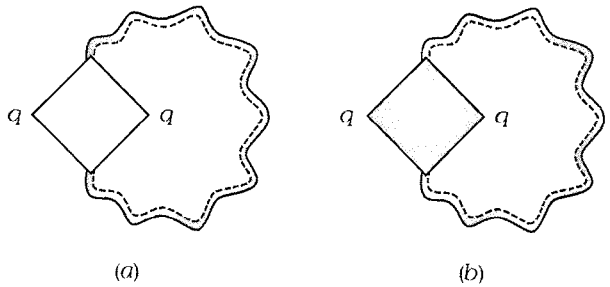

Figure 5. Contribution of the cooperon to the probability a) diagram for $X_c(\mathbf{q},\omega)$. b) Dressing of the Hikami box with impurity lines.

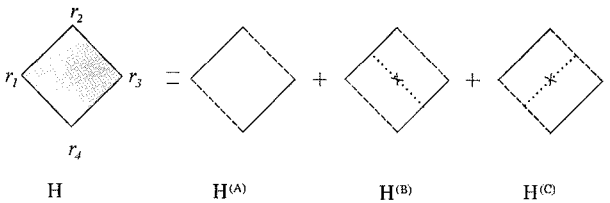

Figure 6. Hikami box.

cooperon will break this normalization. Indeed it appears, as a result of the previous calculation of the cooperon, that the probability is doubled at the origin in a small volume $\lambda^{d-1}l_e$. The relative volume of this enhancement is $\lambda^{d-1}l_e/(Dt)^{d/2}$. It has a maximum for $t \simeq \tau_e$ which corresponds to $1/(kl_e)^{d-1}$. But there exist other terms which contribute as well to the cooperon and which have not been taken into account so far. To identify them, we need to keep in mind the contribution to the cooperon represented by the diagram of Fig. 5. The box describes the interference between four amplitudes. This box can be dressed by one impurity line in two possible ways (Fig. 6). These two additional contributions are of the same order, therefore we should consider the three of them for the full calculation of the cooperon and eventually the normalization of the probability. The first diagram, *i.e.*, the cooperon gives the contribution

$$X_c(\mathbf{r},\mathbf{r}',\omega) = \frac{4\pi}{c} H^{(A)}(\mathbf{r}-\mathbf{r}')\Gamma'(\mathbf{r},\mathbf{r}',\omega) \tag{26}$$

where

$$H^{(A)}(\mathbf{R}) = \left(\frac{l_e}{4\pi}\right)^2 \left(\frac{\sin kR}{kR}\right)^2 e^{-R/l_e} \tag{27}$$

The two other diagrams have a negative contribution which at short distances $r \ll l_e$ is given by

$$H^{(B)}(\mathbf{R}) = H^{(C)}(\mathbf{R}) \propto -\left(\frac{l_e}{4\pi}\right)^2 \frac{1}{kl_e} \frac{\mathrm{Si}(2kR)}{kR} e^{-R/l_e} \tag{28}$$

where Si is the Sine integral function. These two diagrams give indeed at short distances a negligible contribution in comparison to (26). Hence, the return probability to the origin is doubled as obtained before. From the Fourier transforms

$$\begin{aligned} H^{(A)}(\mathbf{q}) &= \left(\frac{l_e}{4\pi}\right)^2 a(q) \\ H^{(B)}(\mathbf{q}) = H^{(C)}(\mathbf{q}) &= -\frac{c^2}{16\pi l_e} a(q)^2 \end{aligned} \tag{29}$$

where

$$a(q) = \frac{\pi}{k^2 q} \left[\arctan(2k - q)l_e + 2 \arctan q l_e - \arctan(2k + q)l_e\right] \tag{30}$$

we obtain that the sum of these three contributions is

$$\int H(\mathbf{R}) d\mathbf{R} = 0 \tag{31}$$

Therefore the contribution of the cooperon which is to enhance the return probability to the origin does not change the normalization of the total probability which is achieved by a small reduction in the wings, *i.e.*, far enough from the origin although of the order of the elastic mean free path l_e.

5. Correlations in Speckle Patterns

Thus far, we have studied the disorder average value of the probability. The averaging procedure is obtained experimentally by considering suspensions of scatterers. An incident wave packet (a pulse) probes a static configuration of the scatterers. This results from the large ratio between the respective velocities of the light inside the medium and of the scatterers. Average quantities are thus obtained through time averaging. Hence, a pulse realizes an instantaneous picture of the disordered medium known as a speckle pattern. This pattern consists in a random distribution of bright and dark spots which signals large fluctuations of the relative intensity. This observation can be made more quantitative and the intensity distribution obeys a Rayleigh law which states that the intensity fluctuations are of the order of the average intensity.

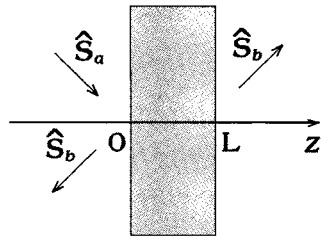

Figure 7. The geometry of a slab of width L and section S used for the measurement of the angular correlation functions both in reflection and in transmission.

There is a large variety of measurements that can be performed to study speckle patterns using electromagnetic waves. The first is given by the angular correlation function either in transmission or in reflection. To that purpose, we consider the slab geometry of Fig. 7. An incident beam along the direction $\hat{\mathbf{s}}_a$ is either reflected or transmitted along the direction $\hat{\mathbf{s}}_b$. We shall be mostly concerned with the transmission coefficient $\mathcal{T}_{ab}$ defined as the intensity $I(R, \hat{\mathbf{s}}_a, \hat{\mathbf{s}}_b)$ transmitted along the direction $\hat{\mathbf{s}}_b$ in the far field, *i.e.*, at a distance R much larger than any of the characteristic dimensions of the slab:

$$\mathcal{T}_{ab} = \frac{R^2}{S} \frac{I(R, \hat{\mathbf{s}}_a, \hat{\mathbf{s}}_b)}{I_0} \tag{32}$$

where I_0 is the intensity of the incoming wave and S is the section of the slab. It is important to notice that this definition differs from those used in the waveguide geometry. In this latter case, the incident and transmitted waves are plane waves with boundary conditions imposed by the waveguide. This gives rise to the quantization of the transverse channels. Here, instead, we have incident plane waves but transmitted spherical waves. This corresponds to different boundary conditions and to a continuous distribution of the transmitted angular directions.

We shall be interested in the normalized correlation function:

$$C_{aba'b'} = \frac{\overline{\delta\mathcal{T}_{ab}\delta\mathcal{T}_{a'b'}}}{\overline{\mathcal{T}}_{ab}\overline{\mathcal{T}}_{a'b'}} \tag{33}$$

where $\delta\mathcal{T}_{ab} = \mathcal{T}_{ab} - \overline{\mathcal{T}}_{ab}$.

By definition, this correlation function is build from the product of complex amplitudes which correspond to all possible multiple scattering sequences in the disordered medium. Like for the calculation of the average

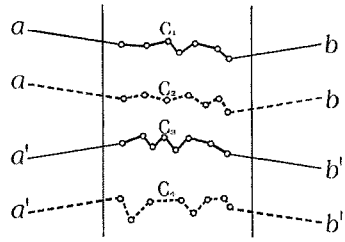

Figure 8. The transmission angular correlation function corresponding to four waves incident along the directions $\hat{s}_a$ and $\hat{s}_{a'}$ and outgoing along the directions $\hat{s}_b$ and $\hat{s}_{b'}$. A non zero contribution corresponds to the pairing of two amplitudes into a diffuson.

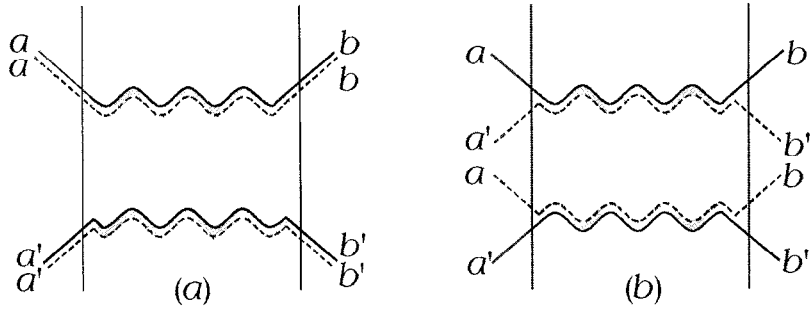

Figure 9. Two contributions to the product $\overline{T_{ab}T_{a'b'}}$ which correspond respectively to the pairing $C_1 = C_2, C_3 = C_4$ and $C_1 = C_4, C_2 = C_3$. The first gives $\overline{T}_{ab}\overline{T}_{a'b'}$. The second corresponds to the angular correlation function noted $C^{(1)}_{aba'b'}$ in the text.

probability, the non vanishing contributions correspond to cases where the amplitudes can be paired into diffusons (see Figs. 8 and 9).

In the case $a = a'$ and $b = b'$, we obtain,

$$\overline{\delta T_{ab}^2} = \overline{T_{ab}}^2 \tag{34}$$

This constitutes the Rayleigh law which accounts for the characteristic granular structure of a speckle pattern, *i.e.*, relative fluctuations of order unity. This is the most important and most "visible" property of a speckle pattern. It exists also in the single scattering regime.

In multiple scattering, there are additional contributions which result from the long range nature of the diffuson and from the existence of cross-

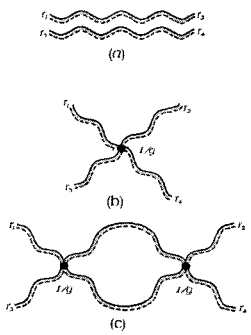

Figure 10. Classification of the contributions to the correlation function $C_{aba'b'}$ in terms of the number of crossings of two diffusons. At each crossing, the corresponding contribution is multiplied by $1/g \ll 1$. These three contributions are respectively denoted $C^{(1)}$, $C^{(2)}$, and $C^{(3)}$.

ings between diffusons. The occurrence of a crossing of two diffusons can be calculated in detail. Let us give first a simple argument. For the slab geometry we consider, the characteristic time for a diffusive trajectory to cross over the sample is $\tau_D = L^2/D$. The length of this trajectory is $\mathcal{L} = c\tau_D = 3L^2/l_e$. The volume of the crossing of two such diffusive trajectories namely the volume of a Hikami box is $\lambda^2 l_e$. We shall thus characterize a diffuson by its length $\mathcal{L}$ and its section λ^2. The occurrence of a crossing of two diffusons is therefore given by the ratio of the two volumes $\frac{\lambda^2\mathcal{L}}{\Omega} = \frac{\lambda^2 L}{l_e S} \propto \frac{1}{g}$, where we have defined the dimensionless quantity

$$g = \frac{k^2 l_e S}{3\pi L} \tag{35}$$

with $k = 2\pi/\lambda$. This is the so-called dimensionless conductance of a wire of length L and section S. In the limit $kl_e \gg 1$ of a weak disorder, g can be very large, typically of order 10^2. Therefore, we may assume that the crossing events are uncorrelated, so that the probability of n crossings is given by $1/g^n$. This allows us to classify the contributions to the angular correlation functions in terms of the number of crossings as represented in Fig. 10.

In order to go further, we need to calculate the average transmission coefficient $\overline{T}_{ab}$. In the slab geometry, it can be written in terms of the structure factor Γ (taken at $\omega = 0$) defined by (17),

$$\overline{T}_{ab} = \frac{1}{(4\pi)^2 S} \int d\mathbf{r}_1 d\mathbf{r}_2 e^{-z_1/\mu_a l_e} e^{-|L-z_2|/\mu_b l_e} \Gamma(\mathbf{r}_1, \mathbf{r}_2) \tag{36}$$

where μ_a (μ_b) is the projection of $\hat{\mathbf{s}}_a$ ($\hat{\mathbf{s}}_b$) along the Oz axis. Moreover, Γ depends on the variables z_1, z_2 and $\rho = (\mathbf{r}_2 - \mathbf{r}_1)_\perp$. Thus, integrating over z_1, z_2 and using the relation (21) in the diffusion approximation, we obtain

$$\overline{T}_{ab} = \frac{c}{4\pi}\mu_a^2\mu_b^2 \int_S d\rho\, P(\rho, l_e, L - l_e) = \frac{c}{4\pi}\mu_a^2\mu_b^2 P(k_\perp = 0, l_e, L - l_e) \quad (37)$$

which depends on the two-dimensional Fourier transform of the diffuson P_d given by (16):

$$P(k_\perp, z, z') = \frac{1}{D}\frac{\sinh k_\perp z_m \sinh k_\perp (L - z_M)}{k_\perp \sinh k_\perp L} \quad (38)$$

with $z_m = \min(z, z')$ et $z_M = \max(z, z')$. For $k_\perp = 0$, we have

$$P(0, z, z') = \frac{z_m}{D}\left(1 - \frac{z_M}{L}\right) \quad (39)$$

Finally, by inserting this relation into (37) we obtain in the limit of small angles $\mu_a \simeq \mu_b \simeq 1$,

$$\overline{T}_{ab} = \frac{3}{4\pi}\frac{l_e}{L} \quad (40)$$

It should be emphasized here that this relation results from a given choice of boundary conditions for the diffusion equation, namely a vanishing of the probability at the boundaries $z = 0, L$ of the slab. A more precise calculation shows that there is an extrapolation length $z_0 \simeq l_e$ at which the probability vanishes outside the medium [1].

5.1. THE SHORT RANGE CORRELATION $C^{(1)}$

The main contribution (*i.e.* without crossing) to the angular correlation function is given by Fig. 9 (b). Its calculation is very similar to those of the average transmission coefficient apart from additional phase factors. We define the vectors $\Delta\hat{\mathbf{s}}_a = \hat{\mathbf{s}}_a - \hat{\mathbf{s}}_{a'}$ and $\Delta\hat{\mathbf{s}}_b = \hat{\mathbf{s}}_b - \hat{\mathbf{s}}_{b'}$ and we neglect their projection along the z-axis so that,

$$\overline{\delta T_{ab}\delta T_{a'b'}} = \left(\frac{1}{(4\pi)^2 S}\int d\mathbf{r}_1 d\mathbf{r}_2 e^{ik[\Delta\hat{\mathbf{s}}_a.\mathbf{r}_1 - \Delta\hat{\mathbf{s}}_b.\mathbf{r}_2]} e^{-z_1/l_e} e^{-|L-z_2|/l_e}\Gamma(\mathbf{r}_1, \mathbf{r}_2)\right)^2 \quad (41)$$

Performing the z-integrals and defining $q_a = k|\Delta\hat{\mathbf{s}}_a|$, we obtain in the limit $q_a l_e \ll 1$,

$$C^{(1)}_{aba'b'} = \delta_{\Delta\hat{\mathbf{s}}_a, \Delta\hat{\mathbf{s}}_b} F_1(q_a L) = \delta_{\Delta\hat{\mathbf{s}}_a, \Delta\hat{\mathbf{s}}_b}\left(\frac{q_a L}{\sinh q_a L}\right)^2 \quad (42)$$

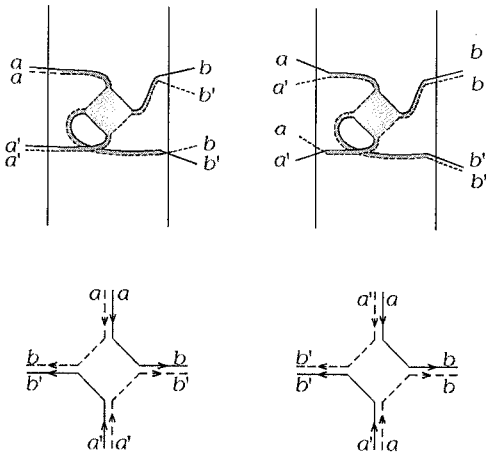

Figure 11. Contribution to $\overline{\delta T_{ab}\delta T_{a'b'}}$ with one crossing. The different cases correspond to configurations of incident plane waves along $\hat{\mathbf{s}}_a$ and $\hat{\mathbf{s}}_{a'}$ and outgoing along $\hat{\mathbf{s}}_b$ and $\hat{\mathbf{s}}_{b'}$. (a) depends on $\Delta\hat{\mathbf{s}}_b$ but not on $\Delta\hat{\mathbf{s}}_a$ and the opposite for (b).

with

$$F_1(x) = \left(\frac{x}{\sinh x}\right)^2 \tag{43}$$

This expression of the angular correlation function allows to understand, at least qualitatively, the *memory effect* [6, 7].

5.2. THE LONG-RANGE CORRELATION $C^{(2)}$

The next contribution to the correlation function arises from terms which involve one crossing of two diffusons. Due to the structure of the Hikami box within which the crossing occurs, the angular correlation function is different from $C^{(1)}$. This is represented in Fig. 11 and it gives rise only to the two possibilities

$$(aa)(a'a') \longrightarrow (bb')(bb') \tag{44}$$

and

$$(aa')(aa') \longrightarrow (bb)(b'b') \tag{45}$$

The corresponding expression for the first one is

$$\overline{\delta\mathcal{T}_{ab}\delta\mathcal{T}_{a'b'}}^{(2)} = \frac{1}{(4\pi)^4 S^2}\int\prod_{i=1}^{4} d\mathbf{r}_i[e^{ik\Delta\hat{\mathbf{s}}_b.(\mathbf{r}_2-\mathbf{r}_4)} + e^{ik\Delta\hat{\mathbf{s}}_a.(\mathbf{r}_1-\mathbf{r}_3)}]E(z_i)$$
$$\int\prod_{i=1}^{4} d\mathbf{R}_i H(\mathbf{R}_i)\Gamma(\mathbf{r}_1,\mathbf{R}_1)\Gamma(\mathbf{r}_3,\mathbf{R}_3)\Gamma(\mathbf{R}_2,\mathbf{r}_2)\Gamma(\mathbf{R}_4,\mathbf{r}_4) \quad (46)$$

where $H(\mathbf{R})$ is the expression of the Hikami box calculated in the diffusion approximation and given by [6, 8]

$$H(\mathbf{r}_1,\mathbf{r}_2,\mathbf{r}_3,\mathbf{r}_4) = \frac{l_e^5}{48\pi k_0^2}\int d\mathbf{r}\prod_{i=1}^{4}\delta(\mathbf{r}-\mathbf{r}_i)\left[2\nabla_{\mathbf{2}}.\nabla_{\mathbf{4}} - {\nabla_{\mathbf{1}}}^2 - {\nabla_{\mathbf{3}}}^2\right] \quad (47)$$

and where we have defined

$$E(z_i) = e^{-(z_1+z_3)/l_e}e^{-|L-z_2|/l_e}e^{-|L-z_4|/l_e} \quad (48)$$

In the diffusion approximation, and using the relation (21), the crossing of two diffusons rewrites

$$\int\prod_{i=1}^{4} d\mathbf{R}_i H(\mathbf{R}_i)\Gamma(\mathbf{r}_1,\mathbf{R}_1)\Gamma(\mathbf{r}_3,\mathbf{R}_3)\Gamma(\mathbf{R}_2,\mathbf{r}_2)\Gamma(\mathbf{R}_4,\mathbf{r}_4)$$
$$= \frac{32\pi^3c^4}{3k^2l_e^3}\int d\mathbf{R}P_d(\mathbf{r}_1,\mathbf{R})P_d(\mathbf{r}_3,\mathbf{R})[\nabla_{\mathbf{R}}P_d(\mathbf{R},\mathbf{r}_2)].[\nabla_{\mathbf{R}}P_d(\mathbf{R},\mathbf{r}_4)] \quad (49)$$

Using the relation (38) to evaluate the gradients and considering the limit $q_b l_e \ll 1$, it remains

$$\overline{\delta\mathcal{T}_{ab}\delta\mathcal{T}_{a'b'}}^{(2)} = \frac{81}{48\pi}\frac{l_e}{k^2LS}F_2(kL\Delta\hat{\mathbf{s}}_b) \quad (50)$$

where we have defined

$$F_2(x) = \frac{1}{\sinh^2 x}\left(\frac{\sinh 2x}{2x} - 1\right) \quad (51)$$

Adding the contribution of the second diagram of Fig. 11, we finally obtain

$$C^{(2)}_{aba'b'} = \frac{\overline{\delta\mathcal{T}_{ab}\delta\mathcal{T}_{a,b'}}}{\overline{\mathcal{T}_{ab}}^2} = \frac{1}{g}[F_2(kL\Delta\hat{\mathbf{s}}_a) + F_2(kL\Delta\hat{\mathbf{s}}_b)] \quad (52)$$

where the conductance g has been defined in (35). This contribution to the correlation function is thus smaller than $C^{(1)}$ by a factor $1/g$. But instead

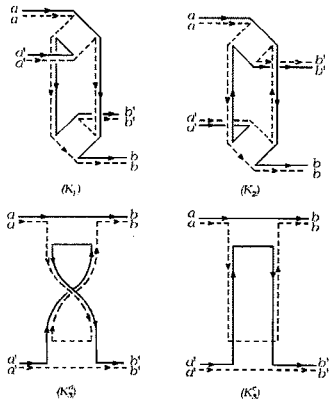

Figure 12. Contributions with two crossings. Those diagrams do not induce angular structure.

of decreasing exponentially, it behaves as a power law and vanishes when both $\Delta\hat{\mathbf{s}}_a$ and $\Delta\hat{\mathbf{s}}_b$ are large.

The next term in the expansion of the angular correlation function in powers of $1/g$ involves two crossings and is represented in Fig. 12. It is thus easy to see that it does not involve any angular structure due to the pairing of the trajectories. The corresponding correlation function thus corresponds to the angular structure

$$C^{(3)}: \qquad (aa)(a'a') \longrightarrow (bb)(b'b') \tag{53}$$

After a calculation similar to those of $C^{(2)}$ but which involves now two Hikami boxes, one finds

$$C^{(3)}_{aba'b'} = \frac{\overline{\delta\mathcal{T}_{ab}\delta\mathcal{T}_{a'b'}}^{(3)}}{\overline{\mathcal{T}}^2_{ab}} = \frac{2}{15}\frac{1}{g^2} \tag{54}$$

But, there exists other contributions to the two crossings term with the angular structure of either $C^{(1)}$ or $C^{(2)}$. They correspond to higher order terms in the $1/g$ expansion of the corresponding correlation functions.

While performing the integration over all the ingoing and outgoing angular directions, only the last term survives so that the relative fluctuations of the total transmission coefficient reduces to

$$\frac{\overline{\delta\mathcal{T}^2}}{\overline{\mathcal{T}}^2} = \frac{2}{15}\frac{1}{g^2} \tag{55}$$

This result is well known in the context of electronic systems as the so-called *universal conductance fluctuations*. There the conductance and the transmission coefficient in a waveguide geometry are related through the Landauer-Büttiker formalism. It is interesting to notice that we have obtained an identical result using a different definition of the transmission coefficient, *i.e.*, a different geometry where the conduction channels do not appear. This is true for the relative fluctuations but is not true anymore for the second moment.

These different contributions associated to the crossings of diffusons have been identified and measured [9]. We shall come back to it in the next section.

6. Diffusive Wave Spectroscopy

We have seen previously that a way to perform disorder averages is to consider suspensions in which the motion of the scatterers provides different realizations of the disorder. Hence the time averaging is equivalent to the averaging over realizations. The measurement of time correlation functions of speckle patterns provides also a very useful tool to investigate the dynamics of the scatterers in the multiple scattering regime. As such it corresponds to a generalization of the quasi-elastic light scattering, a well known experimental tool available in the single scattering regime [10].

We shall be interested in the time correlation functions of the intensity and of the electromagnetic field defined by

$$g_2(T) = \frac{\langle I(T)I(0)\rangle}{\langle I(0)\rangle^2} - 1 \tag{56}$$

and

$$g_1(T) = \frac{\langle E(T)E^*(0)\rangle}{\langle |E(0)|^2\rangle} \tag{57}$$

where the intensity and the field are related as usual by $I(T) = |E(T)|^2$. The notation $\langle \ldots \rangle$ denotes an average over all the multiple scattering sequences in the medium and over the dynamics of the scatterers. We shall assume here that this dynamics corresponds to a non deterministic Brownian motion characterized by a diffusion coefficient D_b (not to be mistaken with the diffusion coefficient $D = \frac{1}{d} v l_e$ obtained previously in the diffusion approximation). Then, the time correlation function of the electric field is expressed in terms of the probability P_d (*i.e.*, the contribution of the diffuson) and using the relation (21) so that

$$\langle E(\mathbf{r},T)E^*(\mathbf{r},0)\rangle = \int_0^\infty dt P_d(\mathbf{r},t) e^{-tT/2\tau_b\tau_e} \tag{58}$$

where the characteristic time $\tau_b = 1/4D_b k^2$ accounts for the motion of one scatterer.

To calculate the intensity correlation function $g_2(T)$, we notice that it involves the average of the product of four electric fields. Hence, using the pairing of these amplitudes as for the calculation of the angular correlation function (see Fig. 9), we obtain [11]

$$g_2(T) = |g_1(T)|^2 \tag{59}$$

In the limit $T = 0$, we recover the second moment of the Rayleigh law, namely $\langle I^2 \rangle = 2\langle I \rangle^2$. From the two expressions (58) and (59) we can deduce the expression of $g_2(T)$. For instance, for the slab geometry using the expression (38) and fixed ingoing and outgoing waves, we obtain a first contribution to $g_2(T)$, usually written as [12, 13]

$$g_2^{(1)}(T) = F_1(L/L_\gamma) = \left(\frac{L/L_\gamma}{\sinh L/L_\gamma} \right)^2 \tag{60}$$

with $L_\gamma = l_e \sqrt{\frac{2\tau_b}{3T}}$. It can be simply deduced from the relation (42) by replacing $1/q_a$ by L_γ.

The relation (59) is a consequence of the absence of crossings of diffusons. We now address the question of the effect of crossings on the time correlation function. The possible pairings of complex amplitudes is represented in Fig. 13. For the one crossing case, we notice that, unlike $g_2^{(1)}(T)$, the corresponding correlation function $g_2^{(2)}(T)$ involves two kind of diffusons, namely those with amplitudes taken at the same time and those taken at the two times 0 and T. The calculation can be done along the same lines as for the angular correlation function $C^{(2)}_{aba'b'}$ with the result

$$g_2^{(2)}(T) = \frac{2}{g} F_2(L/L_\gamma) \tag{61}$$

where the function $F_2(x)$ has been defined previously. We notice, that, unlike $g_2^{(1)}(T)$, this correlation function decreases at large times like a power law. It is nevertheless smaller than $g_2^{(1)}(t)$ by a factor $1/g$, so that its measurement requires to get rid of $g_2^{(1)}(T)$. This can be done by an angular integration over the outgoing directions or equivalently by averaging over a large number of speckle spots [14].

The case of the correlation function $g_2^{(3)}(T)$ which involves two diffusons crossings is more involved. We cannot anymore use the result of the angular correlation function and replace q_a by $1/L_\gamma$ since, as we have seen before,

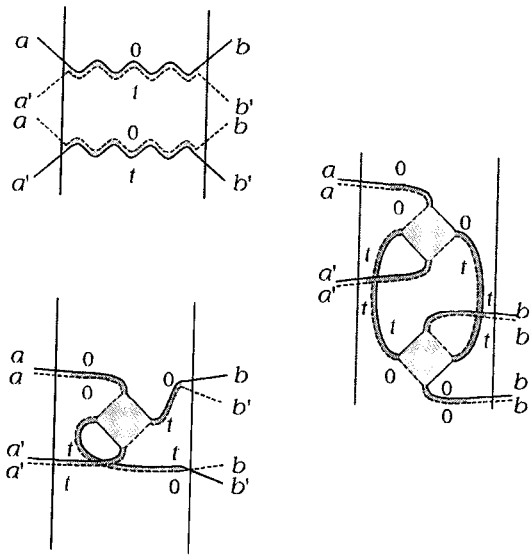

Figure 13. Diagrams contributing to the time correlation functions.

$g_2^{(3)}$ has no angular structure. Using the rules we have previously set for the Hikami boxes and the expression (38) for P_d for the slab geometry, we obtain [1, 15]

$$g_2^{(3)}(T) = \int_0^L \int_0^L dz dz' P_\gamma^2(z, z') = \frac{L^4}{8D^2} F_3(L/L_\gamma) \tag{62}$$

so that

$$g_2^{(3)}(T) = \frac{1}{g^2} F_3(L/L_\gamma) \tag{63}$$

where we have defined

$$F_3(x) = \frac{3}{2} \frac{2 + 2x^2 - 2\cosh 2x + x \sinh 2x}{x^4 \sinh^2 x} \tag{64}$$

We recover the expression $C^{(3)}(0) = 2/15$ for $L_\gamma \to \infty$. The expression of $g_2^{(3)}(t)$ given by (62) involves the integral of P_d^2. This originates from the closed loop which appear in the corresponding diagram of Fig. 13. This expression looks quite close to the one proposed in [9]. But it gives a much slower time dependence which should be sought in the distribution of all closed loops in the slab and not only those touching the boundaries.

The contribution of $g_2^{(3)}(T)$ is much more difficult to observe [9] since it is proportional to $1/g^2 \simeq 10^{-4}$.

In all the three contributions to the time correlation function, we have considered the case of a scalar wave in the absence of absorption. It is justified to treat separately the effect of the polarization of the electromagnetic wave for $g_2^{(1)}(T)$. But it is not anymore the case for the two remaining contributions [15].

7. Dephasing in Cold Atomic Gases

The coherent effects we have presented are very sensitive to dephasing, *i.e.*, to any process which changes the relative phase of the two interfering amplitudes involved in a diffuson or in a cooperon. Roughly speaking, a dephasing may originate either from an external field [16, 17] or from additional degrees of freedom such as the spin-flip scattering in metals where the spin of the electron rotates due to scattering by magnetic impurities or a non deterministic motion of the scatterers such as studied before for the diffusive wave spectroscopy [16, 1]. In the presence of dephasing, the probability of quantum diffusion can be written as $P(\mathbf{r}, \mathbf{r}', t) \left\langle e^{i\phi(t)} \right\rangle$, where the random variable $\phi(t)$ is the relative phase of the two interfering paths. Its distribution depends on the origin of the dephasing and we denote by $\langle ... \rangle$ the average over this distribution. In most cases we have $\left\langle e^{i\phi(t)} \right\rangle \simeq e^{-t/\tau_\phi}$ at least for long enough times t. The characteristic time τ_ϕ is the phase coherence or dephasing time. An exponential decrease of the probability of quantum diffusion does not necessarily describe a dephasing process. For instance, the intensity of an electromagnetic wave which propagates in an absorbing medium decreases exponentially. But this is not a dephasing process since it affects equally both the coherent and incoherent contributions by a decrease of the overall intensity. The propagation of photons in cold atomic gases addresses similar questions and provides new sources of dephasing like internal atomic degrees of freedom. Coherent multiple scattering effects have been observed in such gases and analyzed in great details [18]. The dephasing induced by the internal Zeeman atomic degrees of freedom can be obtained in a closed form [19] in terms of both the polarization state of the photons and of the Zeeman degeneracy.

Each of the N atoms of the gas is taken to be a two-level system of characteristic transition frequency ω_0 [20]. The ground state defines the zero of energy and has total angular momentum J. The excited state has a total angular momentum J_e and a natural width Γ due to coupling to the vacuum fluctuations. We shall assume, moreover, that the velocity v of the atoms is small compared to Γ/k (k is the light wave-vector) but large compared to

$\hbar k/M$ (M being the mass of the atom), so that it is possible to neglect the Doppler and recoil effects. The external degrees of freedom of the atoms are therefore the classical assigned positions $\mathbf{r}_\alpha$ $(\alpha = 1, \ldots, N)$ uncorrelated with one another. The atom-photon interaction is described within the dipole approximation [21], and the elastic scattering process between the two states $|\mathbf{k}\epsilon, Jm\rangle$ and $|\mathbf{k}'\epsilon', Jm'\rangle$, where $|\mathbf{k}\epsilon\rangle$ is a one-photon Fock state of the free transverse electromagnetic field in the mode $\mathbf{k}$ of polarization ϵ, is described by the single scattering transition amplitude $t_{ij}(m, m', \omega) = t(\omega)\langle Jm'|d_i d_j|Jm\rangle$. where the resonant scattering amplitude is given by

$$t(\omega) = \frac{3}{2\pi\rho_0(\omega)} \frac{\Gamma/2}{\delta + i\Gamma/2} \tag{65}$$

with $\delta = \omega - \omega_0$ being the detuning of the probe light from the atomic resonance and $\rho_0(\omega) = \mathcal{V}\omega^2/2\pi^2$ is the free photon spectral density. The average over the disorder is taken over both the uncorrelated positions $\mathbf{r}_\alpha$ of the atoms and over the magnetic quantum numbers m_α of the atoms. The first, standard average restores the translation invariance. The internal average, a trace with a scalar density matrix ρ assuming that the atoms are prepared independently and equally in their ground states, restores rotational invariance. The elastic mean free path is inversely proportional to $t(\omega)$ given in (65). Due to the tensorial structure of the transition amplitude, the diffuson and the cooperon have now three eigenmodes each. The dephasing associated to the internal degrees of freedom affects only the cooperon which is given in the diffusion approximation by

$$X_K(q) \propto \frac{1}{Dq^2 + \tau_d^{-1}(K) + \tau_\phi^{-1}(K)} \tag{66}$$

for $K = 0, 1, 2$. The characteristic times $\tau_d(K)$ are the depolarization times which affect the diffuson as well. They describe the depolarization of the initial light beam and can be calculated in the classical Rayleigh case [22]. The dephasing times associated to the intensity of the field are given by [19]

$$\frac{\tau_\phi(0)}{\tau_{\rm tr}} = \begin{cases} (J(2J+3))^{-1}, & J_e = J+1 \\ J^2 + J - 1, & J_e = J \\ (2J^2 + J - 1)^{-1}, & J_e = J-1 \end{cases} \tag{67}$$

where the transport time $\tau_{\rm tr} = l_e + \Gamma^{-1}$ (in units where $\hbar = c = 1$). An absence of dephasing only occurs for the classical dipole $J = 0$ (Rayleigh scattering) and in the semi-classical limit $J = J_e \to \infty$.

Acknowledgments

This work is supported in part by a grant from the Israel Academy of Sciences, by the fund for promotion of Research at the Technion and by the French-Israeli Arc-en-ciel program. E.A. acknowledges the very kind hospitality of the Laboratoire de Physique des Solides at the university of Paris (Orsay). G.M. acknowledges the very kind hospitality of the Technion.

References

1. E. Akkermans and G. Montambaux, *Propagation cohérente dans les milieux aléatoires: électrons et photons*, EDP Sciences-CNRS (2003) (to be published)
2. E. Akkermans and G. Montambaux, in *"Waves and Imaging through Complex Media"*, P. Sebbah (ed.), Kluwer, Dordrecht, 2001, pp. 29–52 (cond-mat/0104013)
3. S. F. Edwards, Phil. Mag. **3**, 1020 (1958)
4. Notice that we use a notation for $G(\mathbf{r}_i, \mathbf{r})$ where the initial point is on the left and the final point on the right.
5. S. Chakraverty and A. Schmid, Phys. Rep. **140**,193 (1986)
6. R. Berkovits and S. Feng, Phys. Rep. **238**, 135 (1994)
7. I. Freund, M. Rosenbluh and S. Feng, Phys. Rev. Lett. **61**, 2328 (1988)
8. M.C.W. van Rossum and T.M. Nieuwenhuizen, Rev. Mod. Phys. **71**, 313 (1999)
9. F. Scheffold and G. Maret, Phys. Rev. Lett. **81**, 5800 (1998)
10. B.J. Berne and R. Pecora, *Dynamic Light Scattering with Applications to Chemistry, Biology and Physics*, John Wiley, 1976
11. G. Maret and E. Wolf, Z. Phys. **B65**, 409 (1987)
12. P.E. Wolf and Maret, in *Scattering in Volumes and Surfaces*, M. Nieto-Vesperinas and C. Dainty (eds.), North-Holland, Amsterdam, 1990, pp. 37–52
13. D.J. Pine, D.A. Weitz, P.M. Chaikin and E. Herbolzheimer, Phys. Rev. Lett. **60**, 1134 (1988)
14. F. Scheffold, W. Hartl, G. Maret and E. Matijevic, Phys. Rev. **B 56**, 10942 (1997)
15. E. Akkermans and G. Montambaux, in preparation (2002)
16. G. Bergmann, Phys. Rep. **107**, 1 (1984); S. Hikami, A.I. Larkin and Y. Nagaoka, Prog. Theor. Phys. **63**, 707 (1980)
17. B.L. Altshuler, A.G. Aronov and D.E. Khmelnitsky, J. Phys. C **15**, 7367 (1982)
18. G. Labeyrie, F. de Tomasi, J.-C. Bernard, C.A. Müller, C. Miniatura and R. Kaiser, Phys. Rev. Lett. **83**, 5266 (1999), T. Jonckheere, C.A. Müller, R. Kaiser, C. Miniatura and D. Delande, Phys. Rev. Lett. **85**, 4269 (2000) and G. Labeyrie, C.A. Müller, D.S. Wiersma, C. Miniatura and R. Kaiser, J.Opt. **B2**, 672 (2000)
19. E. Akkermans, Ch. Miniatura and C.A. Müller, ArXiv:cond-mat/0206298, to be published
20. C.A. Müller, PhD thesis (Munich/Nice, 2001), unpublished, and C.A. Müller and C. Miniatura, submitted, preprint physics/0205029
21. C. Cohen-Tannoudji, J. Dupont-Roc and G. Grynberg, *Processus d'interaction entre photons et atomes*, Savoirs actuels, InterEditions, Editions du CNRS, (1988).
22. E. Akkermans, P.E. Wolf, R. Maynard and G. Maret, J. de Physique (France), **49**, 77 (1988)